Optical and electron energy loss experiments in ionic $CrBr_3$ crystals

1989 J. Phys.: Condens. Matter 1 7695

(http://iopscience.iop.org/0953-8984/1/41/022)

J. Phys.: Condens. Matter 1 (1989) 7695–7704. Printed in the UK

Optical and electron energy loss experiments in ionic $CrBr_3$ crystals

I Pollini†, J Thomas‡, B Carricaburu§ and R Mamy§

† Dipartimento di Fisica dell' Università di Milano, via Celoria 16, 20133 Milano, Italy

‡ Labratoire de Spectroscopie du Solide (Unitée associée au 1202 CNRS), Faculté des Sciences de l'Université de Rennes I, F-35042 Rennes Cédex, France

§ Laboratoire de Physique des Solides (Unitée associée au 074 CNRS), Université Paul Sabatier, F-31062 Toulouse Cédex, France

Received 28 October 1988, in final form 1 March 1989

Abstract. The fundamental reflectance of $CrBr_3$ crystals has been measured over the energy range 2–31 eV from 300 to 30 K using synchrotron radiation. The high-frequency dielectric tensor elements $\varepsilon_{xx}^{T}(E)$ have been determined by Kramers–Kronig analysis. Energy losses of 50 keV electrons incident along the c axis of the crystal have also been measured up to 30 eV. The results have been described in terms of single-particle excitations (charge transfer, inter-band excitons and transitions) and collective valence electron plasma oscillations. The assignments of direct inter-band transitions both at the critical points Γ and Z and along symmetry lines of the Brillouin zone (Λ line) have been made by considering the intersecting-sphere model calculation of the band structure of $CrBr_3$. The fundamental energy gap, assigned to $\Gamma_3^- \rightarrow \Gamma_1^+$ transitions, at the zone centre is observed around 8.00 eV. Plasma resonance has been observed at 19.8 eV in the electron energy loss spectrum in fine agreement with the maximum of the optical energy loss function. Finally, the fractional ionic character $f_i^{PT} = 0.79$ has been evaluated in the framework of the Phillips dielectric theory.

1. Introduction

In this paper the experimental program on the ultraviolet properties of the transition-metal halides, studied with synchrotron radiation is carried further [1, 2]. Knowledge of the high-frequency dielectric function $\hat{\varepsilon}(E)$ is a powerful method for determining details of the electronic structure of semiconductors and metals especially in connection with band calculations [3]. Apart from a recent investigation of $CrCl_3$ [4, 5], study of the optical properties of chromium halides has been mainly devoted to the low-energy untraviolet region [6, 7] and x-ray photoemission [8]. Since the electronic properties of $CrBr_3$ crystals are not known beyond 9–10 eV, we have decided to study the high-energy spectral region by means of ultraviolet and electron energy loss (EEL) spectroscopies as far as 30 eV [5].

$CrBr_3$ has a hexagonal unit cell with $a = 6.26$ Å and $c = 18.20$ Å [9]. The low-temperature structure of $CrBr_3$ ($T < 450$ K) is the same as the layer-type structure BI_3 (space group, C_{3i}^2). The three-dimensional lattice consists of a stack of sandwiches formed by a hexagonal network of Cr ions between two layers of Br ions, which form cubic close-packed layers on each side of the transition-metal layer. The adjacent

0953-8984/89/417695 + 10 $02.50

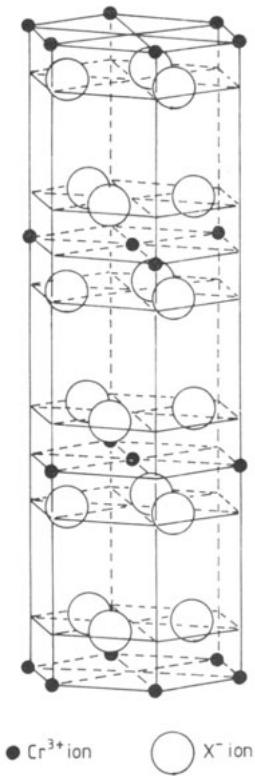

Figure 1. The structure of CrX_3 at low temperatures. The drawing is made from that given in [10].

sandwiches are bonded by weak van der Waals forces, while the bonding is prevalently ionic within the sandwiches (figure 1). A transition to a magnetically ordered state occurs at $T_c = 68$ K [10–12]. Neutron diffraction measurements have established that the magnetisation lies in the direction of the c axis with ferromagnetic coupling between spins.

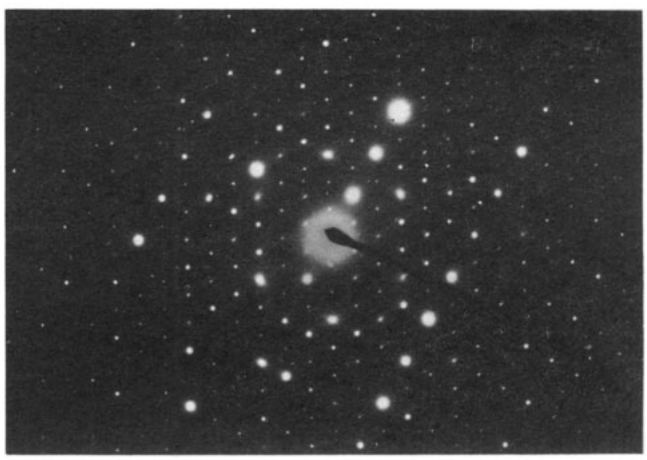

Figure 2. High-energy (200 kV) electron diffraction pattern of crystals of $CrBr_3$.

In the following a brief description of the experimental technique and sample preparation is presented. Then the reflectance and EEL spectra of $CrBr_3$ are presented with the dielectric functions. The real part ε_1 and the imaginary part ε_2 of the dielectric function, together with the optical energy loss function $-\mathrm{Im}[1/\hat{\varepsilon}(E)]$, have been obtained in the region 2–31 eV by Kramers–Kronig (KK) analysis of the near-normal-incidence reflectance spectra. Since $CrBr_3$ crystals are anisotropic and present tensorial dielectric functions, we have measured only the transverse component $\varepsilon_{xx}^{T} = \varepsilon_{yy}^{T} = \varepsilon_{\perp}$ by optical spectroscopy.

2. Sample preparation and experimental technique

The anhydrous form of $CrBr_3$ crystals was prepared with the flow system method at a temperature of about 750 °C. The crystals appear in the form of hexagonal plates with a cleavage plane perpendicular to the *c* axis; they are dark green in colour, lustrous and easy to handle. The thickness of these mica-like platelets of average approximate area 0.8 cm^2 ranges from 5 to 50 μm. The ultraviolet reflectance measurements were made using the radiation provided by the 0.54 GeV electron storage ring of the Laboratoire d'Utilisation du Rayonnement Electromagnétique (Université de Paris-Sud). The monochromator spectral band width was better than 6 Å. The detector set-up was a 9526 S EMI photomultiplier provided with a salicylate phosphor. For the photon flux considered (10^9–10^{10} photon $Å^{-1}\,s^{-1}$) both the scintillator and the photomultiplier used were working in the linearity region.

In all our experiments we investigated the optical reflectance of crystal planes perpendicular to the *c* axis, with the electric vector of the light approximately perpendicular to the *c* axis. The measurements were performed at 300 and 30 K in ultra-high vacuum (10^{-9}–10^{-10} mm Hg). The use of very stable synchrotron radiation incident onto freshly cleaved crystal surfaces permitted excellent reproducibility of the optical data. The samples for EEL and electron diffraction measurements were prepared by stripping them with tweezers, until interference colours indicated a thickness of about 5000 Å suitable for beam transmission. Electron diffraction measurements by means of a Japan Electron Microscope instrument was performed; the results of the Bragg diffraction patterns of 200 keV electrons incident onto the samples are shown in figure 2 and confirm the good crystallinity of the same.

The EEL spectra were obtained by means of an electronic spectrometer, where a monoenergetic electron beam (50 keV) is transmitted through the specimen and is scattered through an angle of 1 mrad [5]. The energy analysis is performed by a cylindrical electrostatic sector with an angle of deflection of $\pi/2\sqrt{2}$. The spectral resolution, defined as the half-width of the elastic peak, is better than 0.5 eV. The apparatus geometry ensures that the momentum transfer and the electric vector for excitation lie in the basal plane of $CrBr_3$ crystals ($\boldsymbol{E} \perp \boldsymbol{c}$).

3. Experimental results

The reflectance spectrum of $CrBr_3$ in the energy range 2–31 eV, together with the dielectric function $\varepsilon_{\perp}(E) = \varepsilon_1(E) + i\varepsilon_2(E)$ and the optical energy loss function $-\mathrm{Im}(1/\hat{\varepsilon})$ is shown in figure 3. This spectrum looks rather similar to that of $CrCl_3$; we still find three characteristic regions, where strong features associated with charge

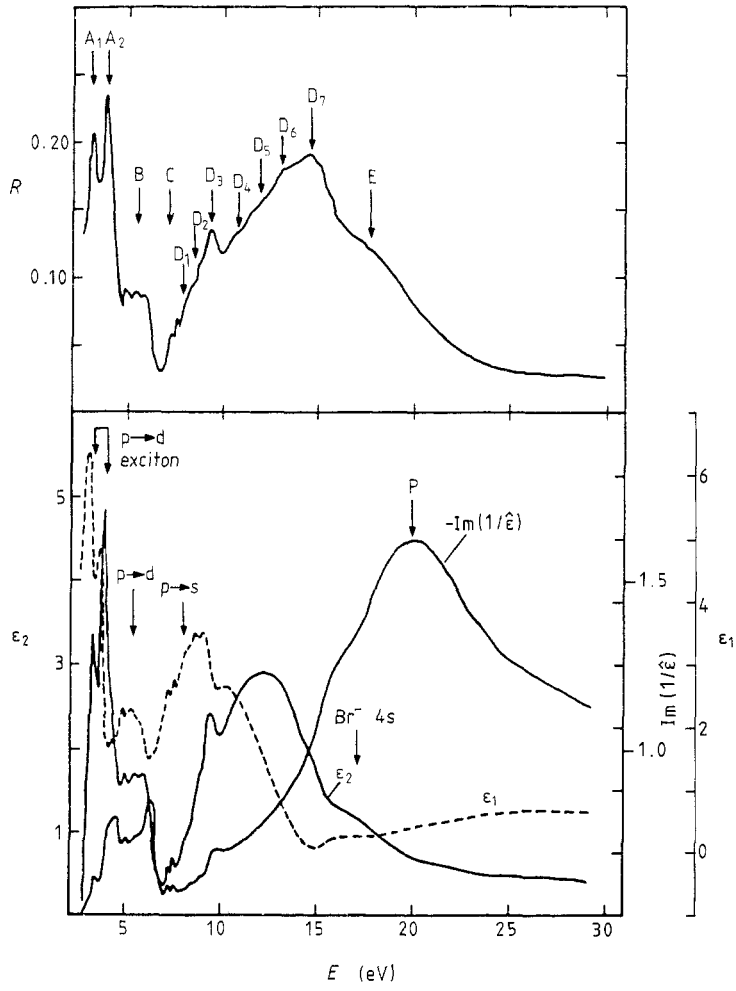

Figure 3. Spectral dependence of the low-temperature reflectance R, the real part ε_1 and imaginary part ε_2 of the dielectric constant and energy-loss function $-\mathrm{Im}(1/\hat{\varepsilon})$ for $CrBr_3$ at 30 K. Peak E at 17.20 eV is due to the excitation of the Br^- 4s shell and peak P at $\hbar\omega_p$ = 20 eV is the plasmon energy measured by EEL spectroscopy.

transfer (CT) excitons (peaks A) and CT transitions (peaks B) occur, followed by strong absorption mainly associated with inter-band excitons and band-to-band transitions (peaks D) and lower atomic excitations (peak E). The higher-energy region between 17 and 31 eV is characterised by a continuous decrease in the reflectance, while the optical function $-\mathrm{Im}(1/\hat{\varepsilon})$ presents a maximum around 20 eV, which can be associated with the existence of plasma oscillations. Direct confirmation of the optical data is shown in figure 4, where the electron loss spectrum of $CrBr_3$ up to 30 eV is presented. The strongest maximum P at 19.8 ± 0.5 eV corresponds to the plasmon energy and is shown to be in fine agreement with the optical results reported below in the figure.

In figure 5 we present the plots $N_{\mathrm{eff}}(E)$ and $\varepsilon_{\mathrm{eff}}(E)$ obtained from the following sum rules:

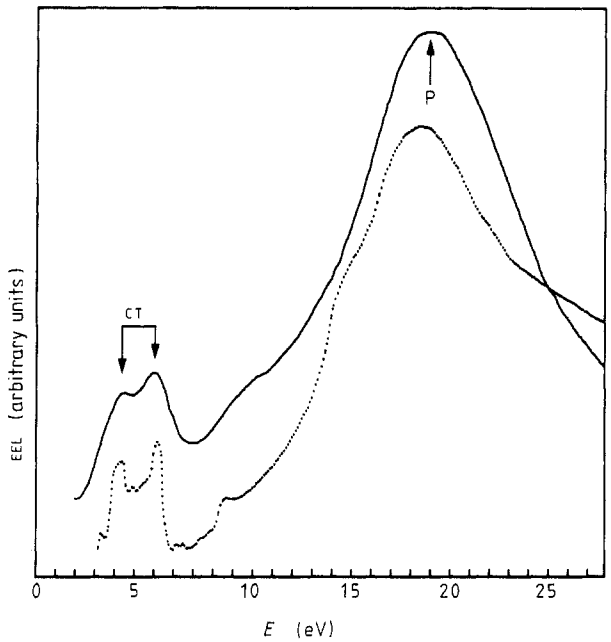

Figure 4. Characteristic EEL spectrum of $CrBr_3$ crystals measured at room temperature (300 K) (——). The energy losses marked CT and P are associated with CT transition and valence electron plasma oscillations respectively. The comparison between electron loss and optical energy loss spectra (- - - -) is shown.

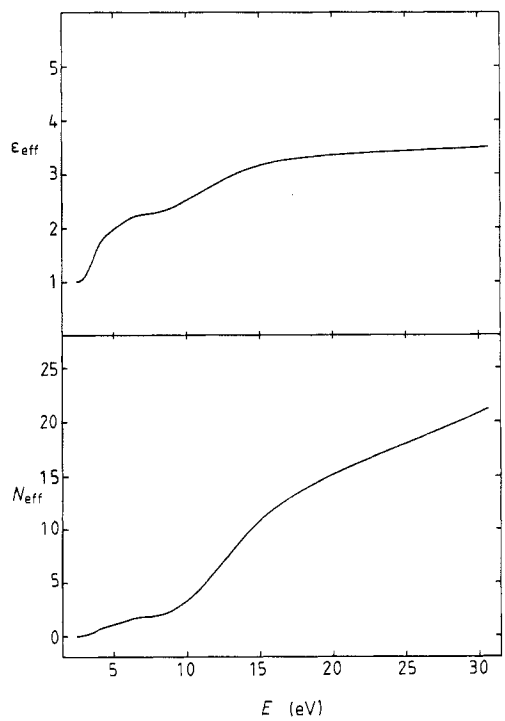

Figure 5. Effective dielectric constant $\varepsilon_{eff}(E)$ and effective number $N_{eff}(E)$ of electrons for $CrBr_3$ at 30 K.

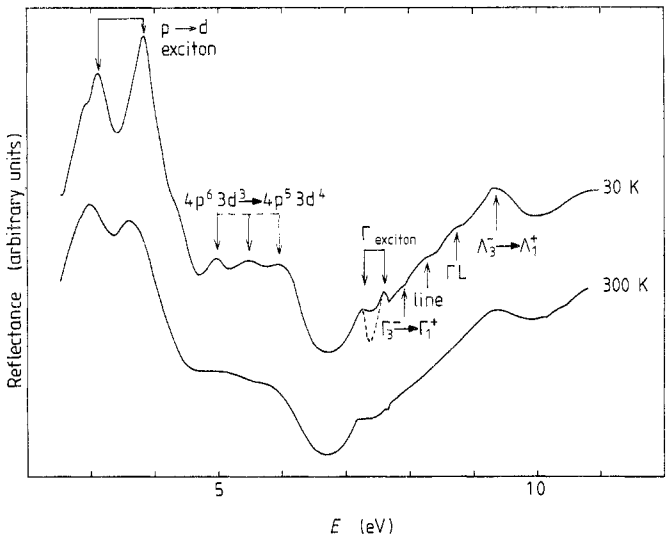

Figure 6. Details of the CT (p → d) and exciton spectrum of $CrBr_3$ in the region of fundamental absorption (p → s).

$$N_{\text{eff}}(E) = \frac{2m\varepsilon_0 V}{\pi\hbar^2}\int_2^E E'\varepsilon_2(E')\,\mathrm{d}E' \tag{1}$$

where m is the free-electron mass, V is the volume of the unit cell (in Å^3), E and E' are in eV and

$$\varepsilon_{\text{eff}}(E) = 1 + \frac{2}{\pi}\int_2^E \frac{\varepsilon_2(E')}{E'}\,\mathrm{d}E'. \tag{2}$$

The effective number $N_{\text{eff}}(E)$ of electrons contributing to the optical absorption at photon energy E should saturate at a value of 27, corresponding to the three d electrons of the Cr^{3+} ion, six 4p and two 4s valence electrons of the Br^- ion. We see that, around 8 eV, N_{eff} begins to increase to high values, reaching the value of 22–23 at 31 eV. We think that the region of low values of N_{eff} (up to two electrons) defines the CT region quite well, while the sudden increase in N_{eff} (around 8 eV) should mark the onset of band-to-band transitions with an optical gap measured at $E_g = 8.00$ eV. The value of the dielectric constant ε_{eff} of $CrBr_3$ determined by the function $\varepsilon_2(E)$ over the entire spectral region saturates beyond 20–25 eV near the value of $\varepsilon_{\text{eff}} = 3.5$, indicating that no further important contributions to ε_{eff} come from the higher-energy transitions.

4. Discussion

The discussion of the complex spectrum of $CrBr_3$ is made on the grounds of the electronic band structure [3] for the intermediate-energy region (from 7 to 15 eV), where joint density-of-states transitions occur. The interpretation of the spectrum of $CrBr_3$ will be made by following closely the similar case of $CrCl_3$ [4].

The optical spectrum of $CrBr_3$ shown in figures 3 and 6 displays strong and sharp structures at low temperatures, which are attributed to excitons connected with both

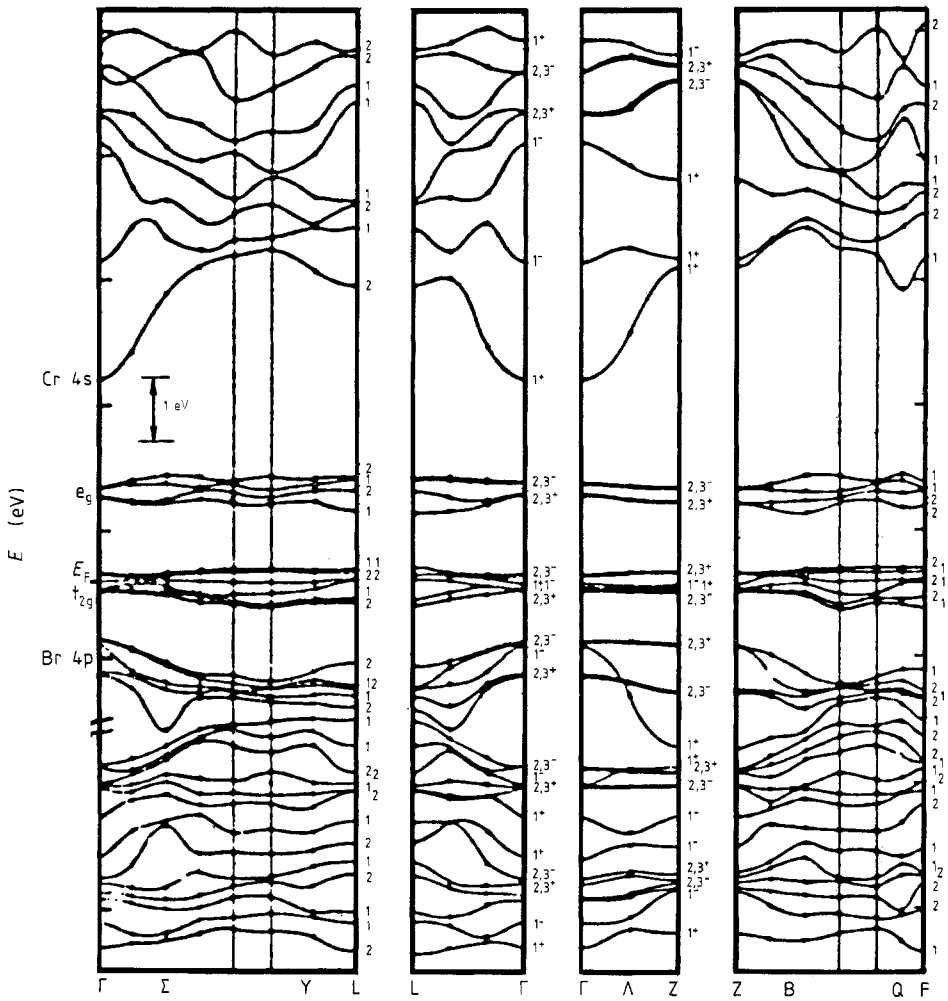

Figure 7. Self-consistent band structure of $CrBr_3$ determined by the intersecting-sphere model according to Antoci and Mihich. The forbidden gap is rigidly shifted in order to reach agreement between the optical gap and the calculated gap considered at the zone centre (Γ). The Fermi level E_F is also reported together with crystal-field notations (t_{2g} and e_g) for the partially filled split 3d band.

p → d CT transitions (peaks A) and band-to-band transitions (peaks D), arising from critical points of the Brillouin zone. The low-energy part of the spectrum, up to 7 eV, due to allowed CT processes has been already discussed in previous work [6].

We observe p → d excitons, bound states of a hole in the 4p valence band, and an extra 3d electron on the Cr state. In this case, the broad and composite absorption band (peaks B) is assigned to the corresponding band part, i.e. leading to unbound states with a hole in the 4p valence band and an extra electron in the 3d band of Cr.

For the discussion of the inter-band transition region, we consider the band structure shown in figure 7. As we have done for $CrCl_3$, the forbidden energy gap between the 4p valence band of the Br and the 4s (Cr) conduction band was rigidly shifted in order to

reach agreement between the optical and the calculated gap considered at the zone centre (Γ).

According to the band-structure calculations, the Cr halides CrX_3 (X = Cl, Br) show a direct energy gap between the halogen p-like band and the s-like conduction band at the Γ point in the Brillouin zone. The uppermost valence band presents maxima at $\Gamma(\Gamma_2^-, \Gamma_3^-)$ and is relatively flat along the symmetry lines ΓZ and ΓL of the Brillouin zone. The lower-lying valence band, associated with Br 4s atomic levels, ranges between -16.5 and -15 eV, below the average d-level position (around the zero of energy). The lowest conduction band is primarily of Cr 4s character with an absolute minimum at $\Gamma(\Gamma_1^+)$. Next in energy, one finds at Γ a Γ_1^- level, associated with Cr 4p orbitals, and another Γ_1^- level predominantly constituted by Cr 4s orbitals. One then finds two groups of six and four bands with very small dispersion (at most 0.3 eV); these levels turn out to be essentially associated with Cr 3d atomic orbitals. Since the crystal potential around each Cr site has approximately octahedral symmetry, these bands are split into two groups of six and four levels, corresponding to the T_{2g} and E_g irreducible representations of the O_h point group. The Fermi level lies within the lower group of bands and the equivalent of three full bands of the lower group is occupied. As in the case of $CrCl_3$, we note that d electrons cannot be described by pure band theory. In effect the properties of Cr 3d electrons cannot be described by the one-electron theory, as developed by Antoci and Mihich, because of large correlation effects between d electrons. For a discussion of the origin of the insulating properties of chromium halides and transition-metal halides in general, we refer to the review article in [13] and the work in [14] introducing the effect of correlation into band theory.

Returning to consideration of the band-to-band region, we note that the first allowed inter-band transitions begin at 8 eV in $CrBr_3$ (D_1 structures) with an Mo-type critical point produced by the $\Gamma_3^- \rightarrow \Gamma_1^+$ transition. The sharp absorption peaks C_1 and C_2 are interpreted as inter-band excitons associated with the inter-band edge $\Gamma_3^- \rightarrow \Gamma_1^+$.

The optical results and the proposed assignments for $CrBr_3$ and $CrCl_3$ crystals are listed in table 1. The fact that band structures of $CrCl_3$ and $CrBr_3$ are very similar to the measured optical spectra provides some help in making reasonably safe attributions in a region where the interpretation of the ultraviolet spectra is necessarily difficult, since several electronic transitions are possible at the same time and the spectra show broad structures. In fact, since the joint density of states for $CrCl_3$ and $CrBr_3$ was not calculated, we can suggest only the most likely assignments for some inter-band transitions beyond the fundamental gaps, which are observed at around 9.50 eV in $CrCl_3$ and 8.00 eV in $CrBr_3$ (D_1 structures). For these reasons, we have given a common discussion of the optical data of Cr halides, listing in table 1 the final attributions.

The optical structure E at 17.20 eV in $CrBr_3$ is assigned to the excitation of the bromide valence 4s shell on the grounds of the atomic energy position of the s levels [3].

The final part of the discussion concerning the calculation of the ionicity parameter f_i^{DT} is given by taking into consideration the observed plasmon energy ($\hbar\omega_p \simeq 20$ eV) and the saturation value of $\varepsilon_{eff} = \varepsilon_1(0) = 3.5$–$3.6$, reported in figure 5. We remark that the value of the experimental plasmon energy is not far from that calculated with the free-electron formula

$$\omega_p^2 = 4\pi ne^2/m \tag{3}$$

where e and m are the electronic charge and mass, respectively, and n is the electronic concentration. We have found that $(\hbar\omega_p)_{FE} = 18.06$ eV with $n = 27$ valence electrons

Table 1. Energies (eV) of the reflectance structures observed at 30 K in layered $CrCl_3$ and $CrBr_3$ crystals in the vacuum ultraviolet range. The suggested assignments are made by considering the original band structures of CrX_3 [3].

Labelling of the peaks	Energy, $CrCl_3$, 30 K (eV)	Assignment	Energy, $CrBr_3$, 30 K (eV)	Assignment
A_1	3.60	p–d excitons	2.90	p–d excitons
A_2	4.70		3.10	
A_3	5.10		3.80	
B_1	6.0	p–d CT	4.95	p–d CT
B_2	6.40		5.40	
B_3	6.85		5.95	
C_1	8.60	Γ excitons	7.20	Γ excitons
C_2	9.20		7.60	
D_1	9.50	$\Gamma_3^- \rightarrow \Gamma_{1,gap}^+$	8.00	$\Gamma_3^- \rightarrow \Gamma_{1,gap}^+$
D_2	10.30	Λ line	8.60	ΓL line
D_3	10.80	Λ line	9.20	Λ line
D_4	12.60	$Z_3^+ \rightarrow Z_1^-$	10.90	Λ line
D_5	13.70	$Z_3^- \rightarrow Z_1^+$	12.00	$Z_3^+ \rightarrow Z_1^-$
D_6	15	$\Gamma_3^+ \rightarrow \Gamma_1^-$	13.00	$Z_3^- \rightarrow Z_1^+$
D_7	—		14.50	$\Gamma_3^+ \rightarrow \Gamma_1^-$
E	17.50		17.20	

per molecule. The correction in [15] of the free-electron formula is

$$(\hbar\omega_p)^2 = (\hbar\omega_p)^2_{FE} + \langle E_g \rangle^2 \tag{4}$$

where $\langle E_g \rangle$ is an 'average energy gap'. The calculated $\langle E_g \rangle$ value obtained from equation (4) gives, for $CrBr_3$, $\langle E_g \rangle = 8.59$ eV. This value can then be used in order to evaluate the fractional ionic character

$$f_i^{DT} = 1 - (E_h/\langle E_g \rangle)^2 \tag{5}$$

where E_h is the homopolar energy gap:

$$E_h = a d_{MX}^{-2.5} \qquad (a = 40.5). \tag{6}$$

The metal–halogen distance d_{MX} is equal to 2.55 Å according to [3, 16]. The calculated ionicity parameter $f_i^{DT} = 0.79$ indicates that $CrBr_3$ crystals are rather ionic material, quite comparable with the $CrCl_3$ crystals ($f_i^{DT} = 0.80$) previously examined [4].

Furthermore, by using the experimental value $\varepsilon_{eff} \simeq \varepsilon_1(0)$ for $CrBr_3$ in order to recalculate the value of $\langle E_g \rangle$ through Penn's formula

$$\varepsilon_1(0) = 1 + (\hbar\omega_p/E_g^{Penn})[1 - E_g^{Penn}/4E_F + \tfrac{1}{3}(E_g^{Penn}/4E_F)^2] \tag{7}$$

where E_F is the Fermi energy in the free-electron model, we obtain a value of $E_g^{Penn} = 10.38$ eV. By using this value of E_g^{Penn} and by following equations (6) and (5), we obtain for $f_i^{DT} = 0.86$†. Finally, we report the ionicity results for CrX_3 halides obtained from a different method of calculation (table 2).

† In [4] it is necessary to correct the value of $f_i^{DT} = 0.85$ by using $(\hbar\omega_p)_{FE} = 19.7$ eV in the Penn formula instead of $\hbar\omega_p = 22.6$ eV as measured; the result is $E_g^{Penn} = 14.29$ eV and $f_i^{DT} = 0.88$.

Table 2. Ionicity results.

$CrCl_3$	$\langle E_g \rangle = 10.9$ eV	$E_g^{Penn} = 14.29$ eV
	$f_i^{DT} = 0.80$	$f_i^{DT} = 0.88$
$CrBr_3$	$\langle E_g \rangle = 8.59$ eV	$E_g^{Penn} = 10.38$ eV
	$f_i^{DT} = 0.79$	$f_i^{DT} = 0.86$

5. Conclusions

Vacuum ultraviolet and EEL spectroscopy have given detailed experimental information about crystalline samples of $CrBr_3$ in the energy range 2–30 eV. The forbidden energy gap $E_g = 8.0$ eV and the plasmon energy $\hbar\omega_p = 19.8 \pm 0.5$ eV have been measured for the first time with good precision for $CrBr_3$. The Phillips–Penn dielectric model has been used to obtain the ionicity coefficient of $CrBr_3$ ($f_i^{DT} = 0.79$). On the grounds of the theoretical band structure and experimental information a new joint interpretation of chromium halides has been given.

Acknowledgments

The authors are grateful to J Ferré for technical assistance and to M Fagot for measuring the electron diffraction pattern of $CrBr_3$ crystals. Three of the authors (I Pollini, J Thomas and R Mamy) thank the technical staff of the Accélérateur Linéaire de L'Université de Paris-Sud for providing the ultraviolet beam during the experiments.

References

[1] Pollini I, Benedek G and Thomas J 1984a *Phys. Rev.* B **29** 3617
[2] Pollini I, Thomas J and Lenselink A 1984b *Phys. Rev.* B **30** 2140
[3] Antoci S and Mihich L 1978 *Phys. Rev.* B **18** 5768
[4] Carricaburu B, Ferré J, Mamy R, Pollini I and Thomas J 1986 *J. Phys. C: Solid State Phys.* **19** 4985
[5] Carricaburu B, Ferré J and Perrier P 1977 *J. Microsc. Spectrosc. Electron.* **2** 39
[6] Guizzetti G, Nosenzo L, Pollini I, Reguzzoni E, Samoggia G and Spinolo G 1976 *Phys. Rev.* B **14** 4622
[7] Nosenzo L, Samoggia G and Pollini I 1984 *Phys. Rev.* B **29** 3607
[8] Okuzawa M, Tsutsumi K, Ishii T and Sagawa T 1982 *J. Phys. Soc. Japan* **51** 510
[9] Handy L L and Gregory W W 1952 *J. Am. Chem. Soc.* **74** 891
[10] Tsubokawa I 1960 *J. Phys. Soc. Japan* **15** 1664
[11] Hansen W N and Griffel M 1959 *J. Chem. Phys.* **30** 913
[12] Hansen W N 1959 *J. Appl. Phys.* **30** 3045
[13] Adler D 1968 *Solid State Physics* **21** 1 (New York: Academic)
[14] Mott N F 1949 *Proc. Phys. Soc.* A **62** 416; 1961 *Phil. Mag.* **6** 287
[15] Horie C 1959 *Prog. Theor. Phys.* **21** 113
[16] Slater J C 1965 *Quantum Theory of Molecules and Solids* vol 2 *Symmetry and Energy Bands in Crystals* (New York: McGraw-Hill)